Available online at www.sciencedirect.com
SCIENCE DIRECT®
PERGAMON
Polyhedron 22 (2003) 2051–2065
POLYHEDRON
www.elsevier.com/locate/poly

Theoretical studies on magnetic interactions in many types of organic donor salts: BEDT-TTF, BETS, TMTTF and TMTSF

Takashi Kawakami *, Takeshi Taniguchi, Shuhei Nakano, Yasutaka Kitagawa, Kizashi Yamaguchi

Department of Chemistry, Graduate School of Science, Osaka University, Osaka 560-0043, Japan

Received 6 October 2002; accepted 7 March 2003

Abstract

Intermolecular magnetic interaction of some donors, i.e. BEDT-TTF, BETS, TMTTF and TMTSF, in some organic superconductive crystals were studied theoretically by using ab initio MO and DFT methods. In addition, donor arrangements in both κ- and λ-phases crystals are also focused. For this purpose we employed κ-$BETS_2FeCl_4$ and λ-$BETS_2FeCl_4$ crystals for BETS salts; κ-$(BEDT\text{-}TTF)_2Cu[N(CN)_2]X$ (X = Cl, Br and I) and κ-$(BEDT\text{-}TTF)_2Cu(NCS)_2$ crystals for BEDT-TTF salts; $TMTTF_2PF_6$ and $TMTSF_2PF_6$ crystals for TMTTF and TMTSF salts. For these systems all the effective exchange integral (J_{ab}) values between two donors and between donor and counter anions were successfully evaluated. In addition the other effective parameters (t_{ab}, U_{eff}) were also obtained. Finally relationship between integral pair (J, J') and transition temperature (T_{SC}) was discussed. The two- and one-dimensional magnetic networks are essential for these crystals.

Keywords: Molecular magnetism; Organic superconductor; Effective exchange integral; Ab initio MO method; Density functional method; BEDT-TTF; BETS; TMTTF; TMTSF

1. Introduction

Past decade, intersection area between molecular magnets and (super)conductors in intermediate or strong electron correlation regimes have attracted much interest in relation to the high-T_c superconductivity in copper oxides [1]. Many experimental and theoretical efforts have been made for elucidation of possible interplay between p- and d-electrons of transition-metal oxides in such regimes. Now it is well established that copper oxides are antiferromagnets before doping, while the species after doping exhibit the high-T_c superconductivity with d-wave symmetry [2–5]. Thus magnetism and d-wave superconductivity is closely related in the species [6].

Many types of important donor-based organic superconductive salts have been reported. The scientific interest in molecular magnets and superconductors with strong electron correlation has been attracted. Specially, even in organic molecular systems these properties have been discovered in many crystals. For such species, some donor molecules, i.e. BEDT-TTF (= bis (ethylenedithio) tetrathiafulvalene), BETS (= bis (ethylenedithio) tetraselenafulvalene), TMTTF (= tetramethyl tetrathiafulvalene), TMTSF (= tetramethyl tetraselenafulvalene) and so on are very important to construct functional complexes (see Fig. 1). The difference between BEDT-TTF and BETS; TMTTF and TMTSF is sulfur (S) and selenium (Se) atoms, which will contribute to intermolecular orbital overlap. In this study we employed these two series of organic donors: BEDT-TTF/BETS and TMTTF/TMTSF, in order to discuss structural one- and two-dimensional interaction in donor layers. In addition, we also discussed contribution of S atoms in BEDT-TTF/TMTTF donors and Se atoms in BETS/TMTSF donors to intermolecular interaction. For these systems many phases of crystal exist, i.e. α, β, κ, λ and θ, and etc. as mentioned Mori's papers. We focus only κ- and λ-phases crystal, though many

* Corresponding author. Tel.: +81-6-6850-5405; fax: +81-6-6850-5550.
E-mail address: kawakami@chem.sci.osaka-u.ac.jp (T. Kawakami).

0277-5387/03/$ - see front matter © 2003 Elsevier Science Ltd. All rights reserved.
doi:10.1016/S0277-5387(03)00298-5

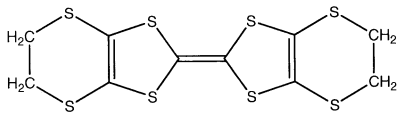

bis (ethylenedithio) tetrathiafulvalene

BEDT-TTF

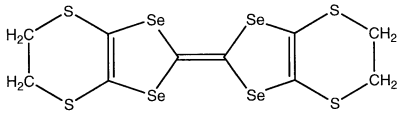

bis (ethylenedithio) tetraselenafulvalene

BETS

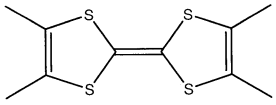

tetramethyl tetrathiafulvalene

TMTTF

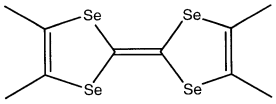

tetramethyl tetraselenafulvalene

TMTSF

κ-$BETS_2X$ (X = $FeCl_4$ (**1a**), $FeBr_4$ (**1b**) and $GaCl_4$ (**1c**))
λ-$BETS_2FeCl_4$ (**2a**)

κ-$(BEDT\text{-}TTF)_2Cu[N(CN)_2]X$ (X = Cl (**3a**), Br (**3b**) and I (**3c**))
κ-$(BEDT\text{-}TTF)_2Cu(NCS)_2$ (**4**)

$TMTTF_2PF_6$ (**5**)
$TMTSF_2PF_6$ (**6**)

Fig. 1. The molecular structure of BEDT-TTF, BETS, TMTTF and TMTSF donors are depicted and those salts which investigated in this paper are listed.

phases exist. Thus, both κ-phase BETS and λ-phase BETS crystals as well as κ-phase BEDT-TTF crystals were employed. Specially, the series of κ- and λ-phases $BETS_2X$ crystals (M = metal atom, X = halogen atom; X = $FeCl_4$ (κ-: **1a**, λ-: **2a**), $FeBr_4$ (κ-: **1b**) and $GaCl_4$ (κ-: **1c**), respectively) show interesting magnetic behavior and are suitable systems for investigation of coexistence of magnetism and conductivity [7–10]. In addition to κ-phase crystals, λ-phase crystals of these salts are useful to study another types of molecular arrangement. Moreover, effective exchange integrals between $BETS^+$ cation and MX_4^- anion are important in order to reveal superconductivity and magnetic features. Thus, several charge transfer salts are very interesting, i.e. κ-$BETS_2FeCl_4$ (**1a**) and λ-$BETS_2FeCl_4$ (**2a**) for BETS salts; κ-$(BEDT\text{-}TTF)_2Cu[N(CN)_2]X$ (X = Cl (**3a**), Br (**3b**) and I (**3c**)) [11,12] and κ-$(BEDT\text{-}TTF)_2Cu(NCS)_2$ (**4**) for BEDT-TTF salts; $TMTTF_2PF_6$ (**5**) and $TMTSF_2PF_6$ (**6**) for TMTTF/TMTSF salts.

For these donors, the effective exchange integrals based on Heisenberg Hamiltonian can describe spin properties, though Hubbard Hamiltonian is also employed to investigate conductive electrons. In series of our studies theoretical calculations by using ab initio molecular orbital (MO) and density functional (DFT) methods were carried out [13]. We have investigated electronic structures of magnetic species on the basis of these spin-polarize methods. In addition, the other effective parameters also evaluated by fitting technique. The J_{ab} values and related parameters indicate the nature of systems. Finally T_{SC} values are also estimated with rough relations between T_{SC} and J_{ab} values.

2. Theoretical background

2.1. Effective exchange integrals (J_{ab}) in Heisenberg model for ab initio calculations

The extended Hückel tight-binding method works well to depict band structures of organic metals [14–18]. However, the band pictures often break down in κ-phase crystals of organic conductors, showing an antifferomagnetic spin order. The magnetism of these CT solids is usually described by the Heisenberg-type spin coupling Hamiltonian

$$H(\mathrm{HB}) = -\sum 2J_{ab}S_a \cdot S_b, \quad (1)$$

where J_{ab} is the orbital-averaged effective exchange integral between the ath and bth metal sites with total spin operators S_a and S_b. Recent development of the ab initio computational techniques has made it possible to calculate the J_{ab} values for organic radical clusters. These methods are classified into two types. One is the spin-symmetry adapted (SA) perturbational and configuration interaction (CI) approach. Use of the SA method is desirable for quantitative computations of J_{ab}, but it is hardly applicable to large organic molecules because of high computational costs. The other is the

broken-symmetry (BS) approach, which is often used for such systems because of lower computational costs, though the spin contamination problem occurs in the low-spin (LS) state. Both spin-projected and unprojected schemes [19] are developed as

$$J_{ab}^{(1)} = \frac{^{LS}E(X) - {}^{HS}E(X)}{^{HS}\langle S^2\rangle - {}^{LS}\langle S^2\rangle} \quad (2)$$

$$J_{ab}^{(2)} = \frac{^{LS}E(X) - {}^{HS}E(X)}{4(N-1)S_aS_b} \quad (3)$$

where $^{Y}E(X)$ and $^{Y}\langle S_2\rangle(X)$ denote, respectively, total energy and total spin angular momentum for the spin state Y by the computational methods X. They are unrestricted Hartree–Fock (UHF) and hybrid DFT methods (UB2LYP and UB3LYP) whose exchange correlation functionals are explicitly given previously [19,20].

Here we defined $J_{ab(M)}$ and $J_{ab(D)}$ as the following. When we evaluate J_{ab} values between two donor molecules in two-dimensional sheets, both $J_{ab(M)}$ (or abbreviated to J_M) values between two donor cations (namely, two holes in two molecules) and $J_{ab(D)}$ (or abbreviated to J_D) values between two donor dimers (namely, two holes in four molecules) are candidate to describe magnetic interaction as shown in Fig. 2A.

For dimer dication and charge-ordered configurations, a simple relation between J_M and J_D is derived,

$$J_D \cong \frac{1}{2}\{J_M(M_1M_3) + J_M(M_1M_4) + J_M(M_2M_3) + J_M(M_2M_4)\} \quad (4)$$

where $J_M(M_iM_j)$ means the effective exchange integral between monomer cation radicals M_i^+ and M_j^+. The J_D values depended on the summation of all J_M values.

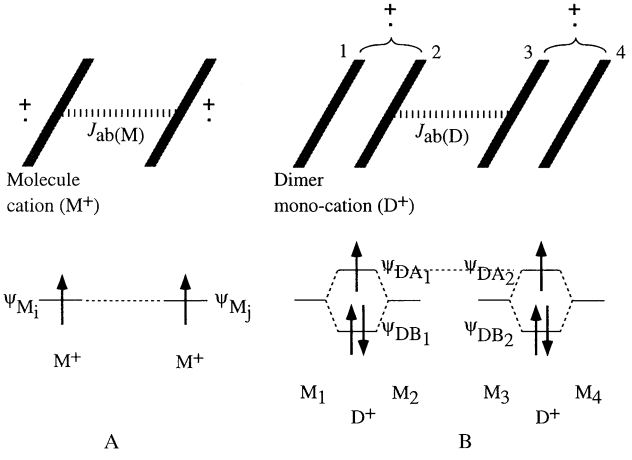

Fig. 2. The $J_{ab(M)}$ and $J_{ab(D)}$ were defined in order to evaluate intermolecular effective exchange integral, where: (A) $J_{ab(M)}$ (or abbreviated to J_M) values between two donor cations (namely, two holes in two molecules); and (B) $J_{ab(D)}$ (or abbreviated to J_D) values between two donor dimers (namely, two holes in four molecules).

On the other hand, the delocalization of an unpaired electron over the dimer cation is often suppressed because of electron correlation, and its localization on one of monomers occurs, leading to the charge-ordered (CO) configuration $(M_1^0M_2^+ - M_3^+M_4^0)$ and $(M_1^+M_2^0 - M_3^0M_4^+)$. The effective exchange interaction (J_D(CO)) between CO dimer cations is reduced to that of molecules M_2 and M_3 if the localization is complete.

$$J_D(CO) \cong \begin{cases} J_M(M_2M_3) \\ 0 \end{cases} \quad (5)$$

However, the intermediate situation between completely delocalized and localized limits is realized in organic CT solids. If CO configuration is suppressed and the delocalization of an unpaired electron is achieved, we can use relation the following to evaluation J_D from J_M values. Here, we assume that $J_M(M_2M_3)$ has main contribution to magnetic interaction among four J_M terms.

$$J_D \equiv \frac{1}{2}\, J_M(M_2M_3) \quad (6)$$

2.2. Effective parameters (t_{ab}, U_{eff}) in Hubbard model

Hubbard Hamiltonian is usually employed in order to investigate electronic properties for copper oxide and organic superconductor, though Heisenberg Hamiltonian is also effective to describe localized quantum spin properties as discussed our previous papers [21].

$$H_q = \sum\, t_{qq}a_q^+a_q + \sum\, U_{qp}a_q^+a_qb_r^+b_r(q,\ r = p\ \text{or}\ d)$$
$$H_{pd} = \sum\, t_{pd}(a_p^+b_d + a_d^+b_p), \quad (7)$$

where a^+ and b^+ create electron (or hole) on the ith a site and the jth b site, respectively. U_{aa} and U_{ab} ($= V_{ab}$) are on-site and inter-site Coulomb repulsion, and t_{aa} ($= \varepsilon_{aa}$) and t_{ab} are orbital energy and transfer integral, respectively. Imamura et al. [22] and Fortunelli and Painelli [23] already calculated these integrals by using restricted Hartree–Fock (RHF) methods and other scientists also evaluated them with other methods [24,25]. The parameters were estimated from the ab initio results and spectroscopic data as shown previously. The Hubbard model often reduces to the Heisenberg spin Hamiltonian in the case of strong electron systems. The exact diagonalization (full CI) of singlet and triplet CI matrices of the Hubbard model provide the effective exchange integral as

$$2J_{ab} = \frac{1}{2}[(U_{aa} - V_{ab}) - \sqrt{(U_{aa} - V_{ab})^2 + 16t_{ab}^2}] \quad (8a)$$

$$\cong -4\frac{t_{ab}^2}{U_{aa} - V_{ab}} \tag{8b}$$

$$= -\frac{4t_{ab}^2}{U_{eff}}. \tag{8c}$$

If the effective exchange integral between radical clusters is weak, it can be approximately given on the basis of the perturbation theory.

The parameter sets (U_{aa}, V_{ab}, t_{ab}) in the Hubbard models can be determined using several experimental data, together with ab initio computational results such as J_{ab} values for magnetic clusters. Both ab initio and semiempirical calculations have been performed to determine reasonable parameters of the Hubbard models. For example, t_{ab} is estimated by using the orbital overlap integral between SOMO(a) and SOMO(b),

$$t_{ab} = \beta s_{ab} \tag{9}$$

where β is a fitting parameter for ab initio results or experiments.

In order to reproduce effective parameters with parameter fitting easily, U_{eff} is also introduced with both J_{ab} and s_{ab} in the following section. These integrals lead the formulation for J_{ab} and especially Eq. (8a) can be reduced in the case of small parameter t_{ab} with pertubation technique, where transfer integral is defined by Eq. (9). We define effective parameters U_{eff} ($= U_{aa} - V_{ab}$) and Eq. (8a) can be re-written to as the following.

$$J_{ab} \equiv \frac{1}{4}[U_{eff} - \sqrt{U_{eff}^2 + 16s_{ab}^2\beta^2}]. \tag{10}$$

2.3. Estimation of transition temperature (T_c) with effective exchange integrals

Previously the four-component spinor (Nambu expression) was introduced to characterized possible electronic phases of molecular materials: (1) charge density wave (CDW); (2) spin density wave (SDW); (3) singlet superconductor (SSC); (4) triplet superconductor (TSC); and (5) ferromagnetic metal (FM). The phase diagrams of these states were depicted using two-band model in combination of the temperature Green function technique. Our theoretical investigations elucidated four different approaches to obtain high-T_c superconductors in the intermediate regime of the metal insulator transitions. One of them is an approach from the strong correlation limit using the resonating valence bond (RVB) and the other is a spin-fluctuation model from the metallic side: these were referred to as the unified J-model as illustrated in Fig. 3A.

Our unified J-model was extended so as to reproduce experimental results on the basis of Ginsburg–Landau (GL) model. The transition temperatures for antiferromagnetic (AF) and SSC phases were given by

$$T_C(\mathrm{AF}) \propto J(x_{min} - x) \tag{11a}$$

$$T_C(\mathrm{SSC}) \propto J(x - x_{min})(x_{max} - x) \tag{11b}$$

where x is the hole concentration, and x_{min} and x_{max} are its lower and upper limits for SSC. The transition temperature (T_c) for AF phase decreases with the increase of x ($x < x_{min}$), while T_c (i.e. superconductive transition temperature (T_{SC})) for SSC has the maximum in the intermediate region ($x_{min} < x < x_{max}$). The origin of the high-T_c superconductivity of copper oxides is regarded as strong effective exchange interaction ($2|J| > 1000\ \mathrm{cm}^{-1}$).

Through this study, ab initio and DFT methods can successfully evaluate J_{ab} values. Here, we study the temperature of superconductive transition for our advanced discussion. Simple equation to estimate T_{SC} was proposed and the relationship between J and T_{SC} values is

$$T_{SC} \propto \sqrt{J \times J'}(x - x_{min})(x_{max} - x) \tag{12}$$

Here, J and J' are effective exchange integrals on two directions and x is hole densities,

3. Crystal structures and molecular orientations for employed complexes

As mentioned in our introduction section, the salts with BETS, BEDT-TTF, TMTTF and TMTSF donors are very familiar and important and they have been reported by many scientists. Very noble and important superconductive properties are achieved in the series of these salts [7,11,12]. Particularly in κ-/λ-phases BETS salts magnetic couplings as well as superconductive properties are also important.

The κ- and λ-phases crystal of BETS salts and κ-phase crystal of BEDT-TTF salts have similar crystalline structure and simple representation is depicted in Fig. 4A, though the space group and cell constants for each system are different each other. In this figure, it is found that two-dimensional donor layers and their counter ions layers exist alternatively. First, let us start our discussion on the crystals of κ-phase BETS salt. The κ-phase crystal of **1a**, which was employed mainly in this paper, has the unit cells classified by a space group of *Pnma* (62) and its cell parameter sets are ($a = 11.693$, $b = 35.945$ and $c = 8.4914$ Å) [26]. Here we employ the X-ray structural study measured in room temperature ($T = 295$ K) as experimental condition, although we have to empory the structural data for lower temperature and it is our future study. This salt consists of both layers of donor molecules (BETS) and counter anions (transition metal halides: $FeCl_4$). The more detailed molecular arrangement between each BETS molecule in two-dimensional sheets is depicted in Fig. 5A and eight

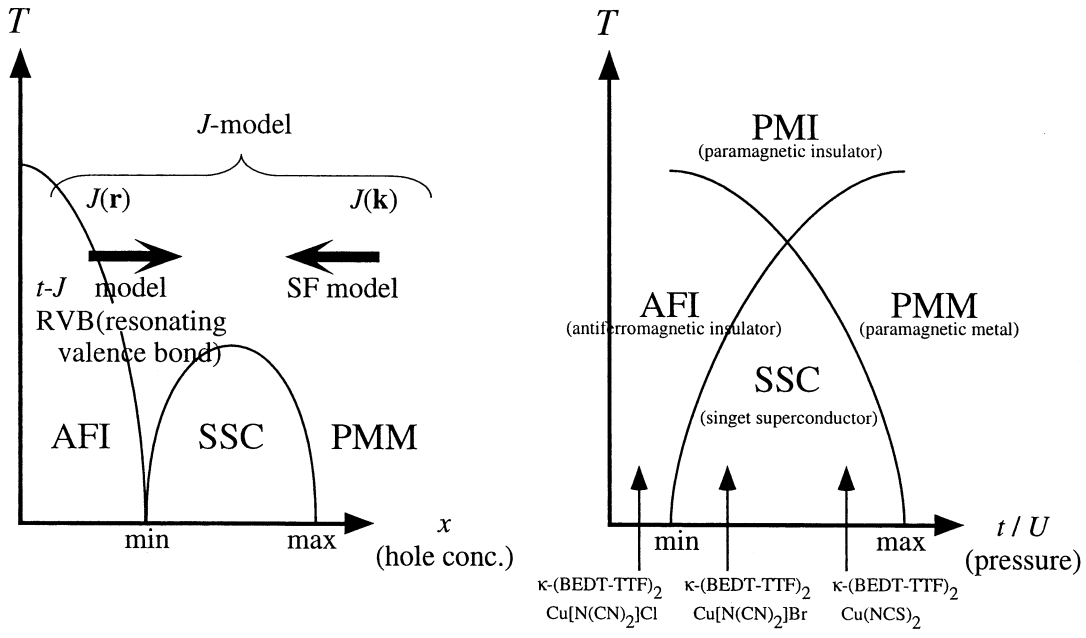

Fig. 3. (A) The phase diagram for superconductive species and the way to approach for superconductive region are illustrated. (B) The phase diagram for several κ-phase BEDT-TTF salts.

molecules 1, 2, 3, 4, 5, 6, 7 and 8 are indicated. Especially, the molecules 1 and 2 contact each other with close face-to-face type stacking and realize dimer structure. Parameters A ($=1$–2), B (2–5), p (2–7) and q (2–8), which had been introduced in the previous Hotta's [27] and Mori's [18] papers, were defined to indicate magnetic couplings between two molecules (as $J_{ab(M)}$). Each circle indicates dimer structures of molecules and parameters 1, 2 and 3 were defined to indicate magnetic interaction between two dimers (as $J_{ab(D)}$). In addition to spatial arrangement of donor molecules, the detailed molecular arrangement between donor and

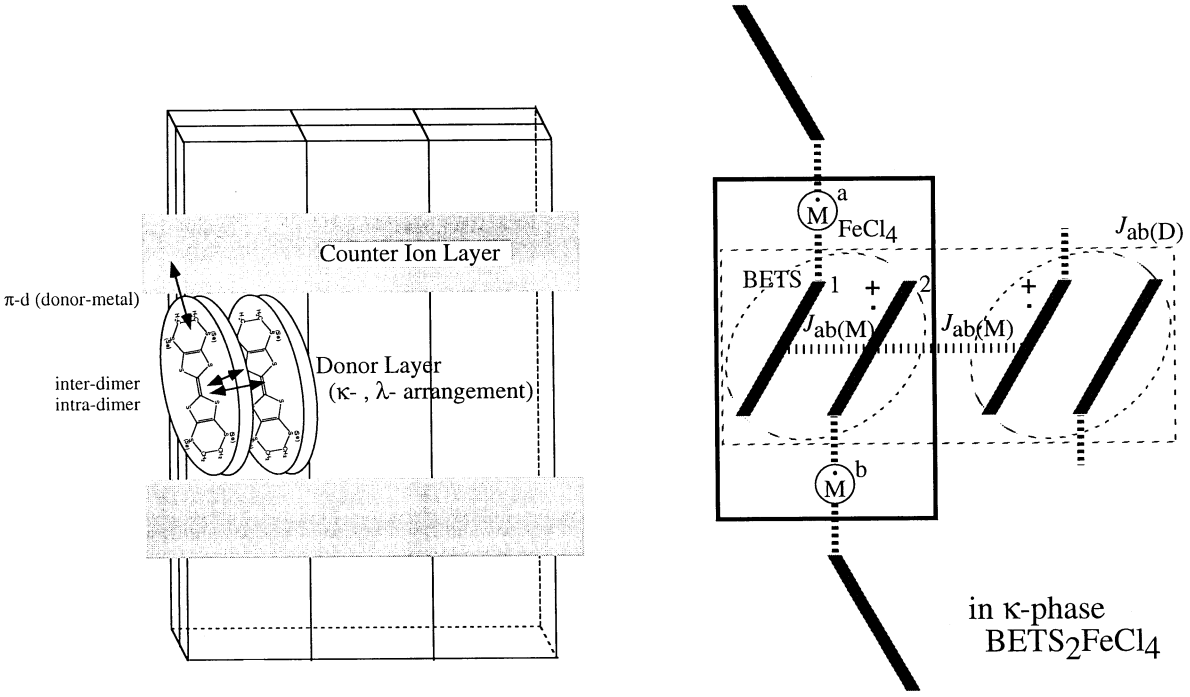

Fig. 4. (A) The crystal structure of donor complexes which consist of donor and counter ion layers is illustrated. (B) The magnetic coupings between donor and counter anions are simply illustrated.

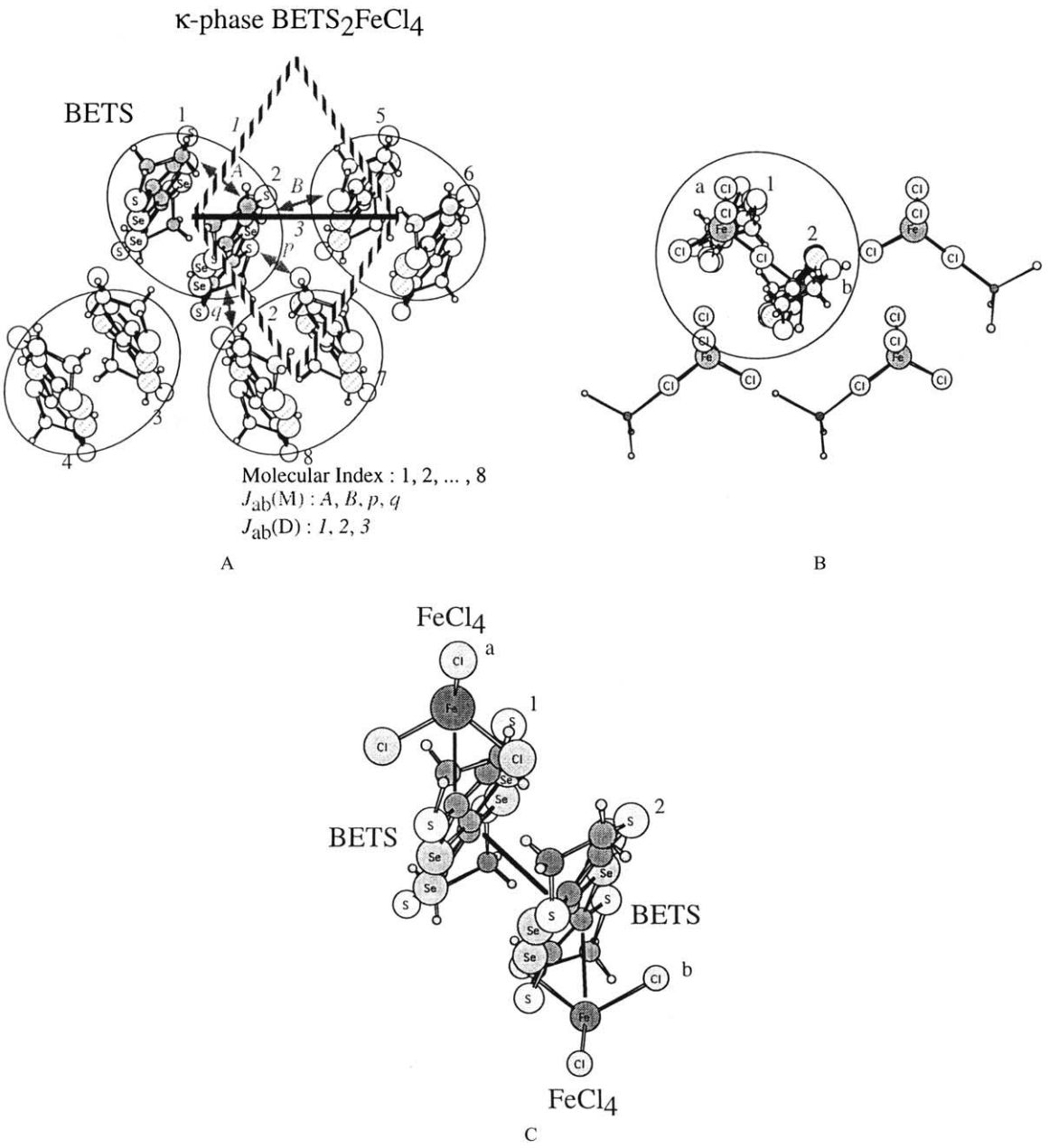

Fig. 5. For κ-phase $BETS_2FeCl_4$, (A) orientations and indexes for BETS molecules in donor layer and (B) orientations for $FeCl_4$ molecules in counter ion layer are illustrated. (C) The nearest neighbor orientations between BETS and $FeCl_4$ molecules are illustrated.

counter anions is depicted in Fig. 5B. Especially, molecular cluster of molecules 1 and 2 ($BETS^{(+,0)}$ donor), a and b ($FeCl_4^-$ anion) will interact strongly and is depicted in Fig. 5C. In this paper, we first started our investigation from treating only the layer of BETS donors as shown in Fig. 5A. Next, in order to sttudy contribution of $FeCl_4^-$ anions to magnetic couplings we studied interaction between donors and counter anions as shown in Fig. 5C. The all interaction paths as shown in Fig. 4B were taken into account in our following calculations.

For the λ-phase crystal of BETS salts, spatial relation among these molecules have another type arrangement to κ-phase crystals. In Fig. 6A and B crystal structure of **2a** are depicted for relationship between each BETS donor and between BETS donor and $FeCl_4^-$ counter anions, respectively. It is found that molecular orientation in this λ-phase structure differ from the κ-phase crystals. The complexes have the unit cells classified by a space group of $P\bar{1}$ (2) and cell parameter sets are ($a = 16.164$, $b = 18.538$, $c = 6.5928$ Å, $\alpha = 98.40$, $\beta = 96.67$ and $\gamma = 112.52°$). Here we also employ the X-ray structural study measured in room temperature ($T = 295$ K) as experimental condition. In two-dimensional stacking of BETS molecules 1, 2, 3, 4, 5, 6, 7, 8, 9 and 11 are indicated. In this figure dimer structure is also

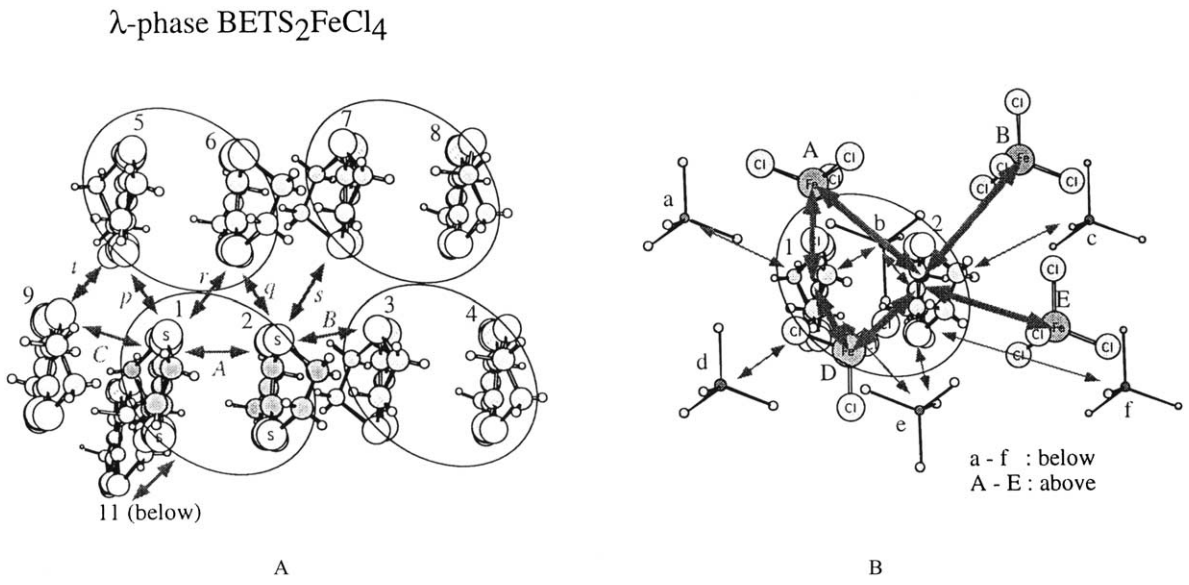

Fig. 6. For λ-phase $BETS_2FeCl_4$, (A) orientations and indexes for BETS molecules in donor layer and (B) orientations between BETS and $FeCl_4$ molecules and their indexes are illustrated.

expected, though the structural deformation derived from dimerization is small. The encircled two BETS molecules will interact each other tightly.

Next, the relation between each BEDT-TTF molecule in two-dimensional layers in κ-phase crystals were also taken into account and both arrangement for BEDT-TTF and BETS clusters resemble each other. For the series of κ-phase crystals of BEDT-TTF salts have the unit cells classified by a space group of *Pnma* (62) for **3a**, **3b** and **3c** as same as **1a**, P21 (4) for **4**. For example, the κ-phase crystal of **3b** has cell parameter sets ($a = 12.878$, $b = 29.681$ and $c = 8.484$ Å) [28,29]. Here we employed the X-ray structural studies measured in $T = 127$ K for **3a**, **3b** and **3c**, $T = 295$ K for **4**. In Fig. 7 the more detailed molecular orientation in two-dimensional layers of BEDT-TTF molecules in κ-phase crystal of **3b** is depicted and eight molecules 1, 2, 3, 4, 5, 6, 7 and 8 were indicated. In addition, intermolecular indices A (=1–2), B (2–5), p (2–7) and q (2–8) were also shown as well as those in the κ-phase BETS salts. From Fig. 5A and Fig. 7 it is commonly found that each molecule in both κ-phase BETS and BEDT-TTF salts has resemble spatial orientation. The other crystals **3a**, **3c** and **4** were also employed to evaluate the detailed intermolecular magnetic interaction. For these crystals Fig. 3B illustrates the phase diagrams at ambient pressure. The previous papers by the other scientists said that crystals **3b** and **4** are superconductors like many other organic superconductors. On the other hand, **3a** is a paramagnetic insulator (PMI), but an antiferromagnetic insulating (AFI) phase is stabilized below $T_N = 27$ K at ambient pressure. With increasing pressure, the Neel temperature of AFI is suppressed and the SSC phase appears. The SSC transition temperature of **3a** takes its

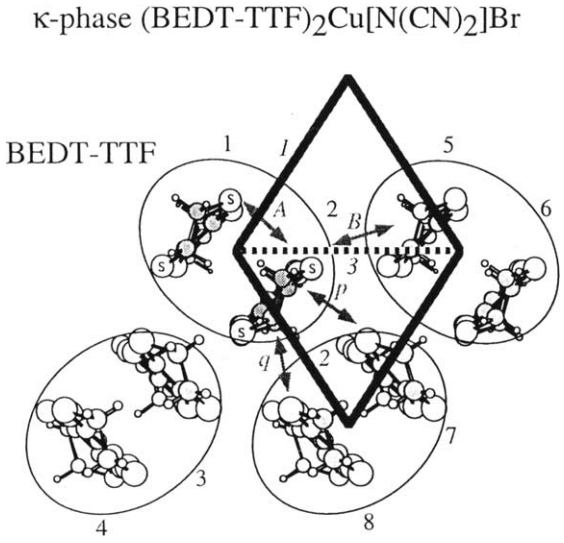

Fig. 7. For κ-phase $(BEDT\text{-}TTF)_2Cu[N(CN)_2]Br$, orientations and indexes for BEDT-TTF molecules in donor layer are illustrated.

maximum value ($T_{SC} = 13$ K) at 300 bar, but the SSC phase is also suppressed under high pressure, giving rise to paramagnetic metal (PMM) phase. Nevertheless, we could not find remarkable differences among these crystals and used these compounds without special treatments.

Finally, for TMTTF and TMTSF donors, one-dimensional organic complexes **5** and **6** were employed. In Fig. 8A the unit cells for both **5** and **6** are depicted in same figure. These structural data were given by neutron diffraction measurements at $T = 4$ K. In this temperature it was reported that spin-Peierls transition occurs and small dimerization is found, though the structural

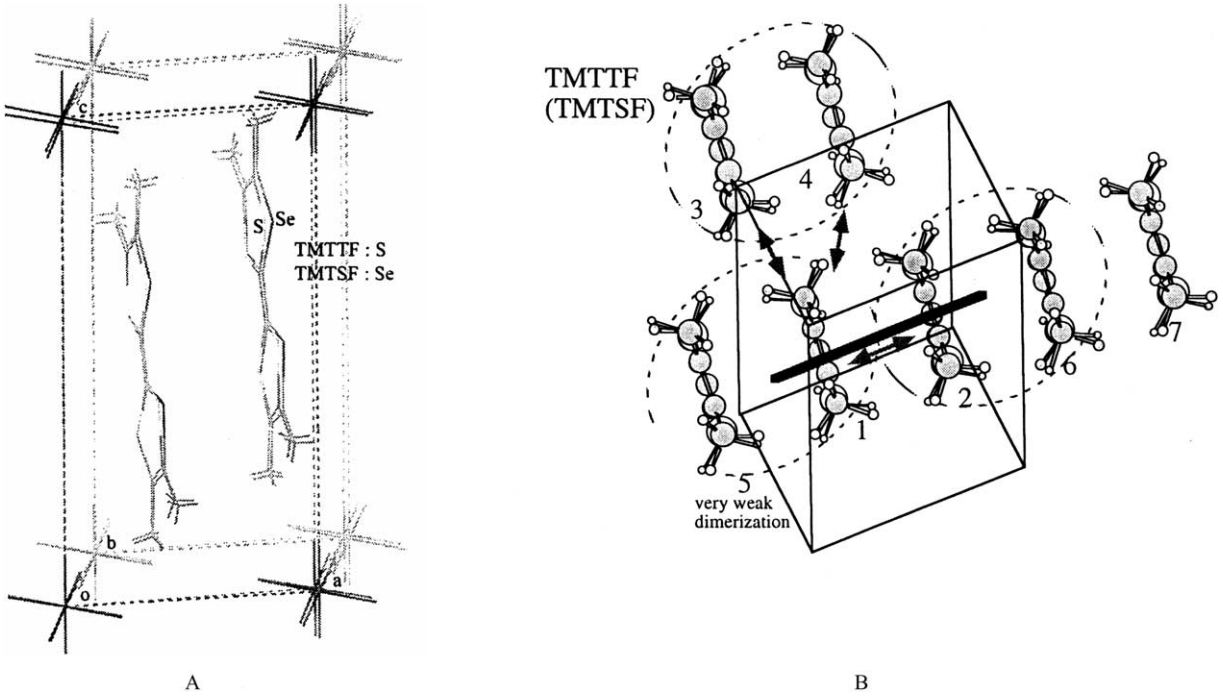

Fig. 8. (A) The unit cell of $TMTTF_2PF_6$ and $TMTSF_2PF_6$ crystals are showed in same figure. (B) Orientation and indexes for TMTTF molecules in donor layer are illustrated.

alternation derived from dimerization is hardly found. The complexes **5** have the unit cells classified by a space group of $P\bar{1}$ (2) and cell parameter sets are ($a = 6.936$, $b = 7.508$, $c = 13.045$ Å, $\alpha = 83.71$, $\beta = 87.20$ and $\gamma = 70.81^\circ$). The detailed molecular arrangement between each TMTTF molecule is depicted in Fig. 8B for **5** and five molecules 1, 2, 3, 4, 5, 6 and 7 are indicated. Similar structure is also found in **6** as the TMTSF salts.

4. Detailed theoretical calculations

4.1. Computational methods

In this paper, the effective exchange integrals based on Heisenberg Hamiltonian can describe spin properties, though Hubbard Hamiltonian is also employed to investigate conductive electrons. In series of our studies theoretical calculations by using ab initio molecular orbital (MO) and density functional (DFT) methods were carried out. We calculated J_{ab} values for dimer dications of organic donors by these methods. Implications of the calculated results are discussed in relation to superconductivity of organic charge-transfer (CT) salts.

Previously we have investigated electronic structures of undoped copper oxides on the basis of spin-polarized HF (UHF) [30], DFT (UDFT) and hybrid DFT approximations [20]. In order to investigate antiferromagnetic phase of transition metal oxides and halides, we have calculated the J_{ab} values between transition metal ions using these computational methods. The spin-mediated superconductivity has been also proposed on the basis of large J_{ab} values for copper oxides, and the transition temperature is simply estimated by $T_{SC} = cJ_{ab}$ (c = constant (= 0.1)) [30]. As an extension of our J model [6,30], we here investigate organic superconductors on the basis of the localized picture instead of the band picture [17,18].

Before our treatment of theoretical calculation, we examined basis set dependency. Thus, we use the simple basis sets included in GAUSSIAN-98 program packages.[31] Moreover, actual calculations were carried out for typical donor pairs in BETS, BEDT-TTF and TMTTF salts and these results by using of several basis sets are summarized in Table 1. From these results all basis sets except for the STO-3G basis sets can reproduce large antiferromagnetic interaction. Polarization function and diffuse functions improve magnetic interaction slightly. Thus, it is concluded that our selection of the 6-31G basis set is suitable for these case. When we evaluated interaction between donor and counter ions, MIDI ((53 321/53/41)+4p for Fe) basis sets were also used.

4.2. BETS complexes

4.2.1. For κ-phase crystal in $BETS_2FeCl_4$

When we evaluate J_{ab} values between two donor molecules in two-dimensional sheet, both $J_{ab(M)}$ values between two $BETS^+$ cations and $J_{ab(D)}$ values between

Table 1
Basis set dependency for the evaluated $J_{ab(M)}$ (cm^{-1}) values in donor pair (1–2) in each complex

	κ-$BETS_2FeCl_4$		κ-(BEDT)$_2$TTF)$_2$Cu-[N(CN)$_2$]Br	$TMTTF_2PF_6$
Basis set	UHF	UB3LYP	UHF	UHF
STO-3G	−55.3	−370.6	−44.4	−31.5
3-21G	−287.0	−848.6	−283.3	−241.4
4-31G			−251.0	−223.5
6-31G	−263.8	−821.8	−279.6	−244.9
6-31G*	−270.8	−848.5	−297.0	−252.7
6-31G**	−270.7	−848.3	−297.1	−253.4
6-31+G	−276.1			−265.3
6-31++G				−265.0

two BETS dimers are candidate to describe magnetic interaction as shown in Fig. 2A and B. In this section we first start to evaluate $J_{ab(M)}$ values with several ab initio theoretical calculations.

In this section, we focused on cation radical dimer of BETS salts in order to evaluate J_{ab} values, though studies for many BEDT-TTF salts will be discussed in the following. First, let us study κ-phase of BETS salts with $FeCl_4$ as counter ions whose crystal structure studied in 295 K.

Their molecular structures and notation for each molecule are illustrated in Fig. 5A schematically. First, we have calculated the J_{ab} values in the layers of molecular cations. All calculations were also performed by using GAUSSIAN-98 program package. The spin-projected scheme by Eq. (2) was applied to effective exchange integrals.

We calculated the $J_{ab(M)}$ values between two BETS donor (namely, two holes in two molecules) in two-dimensional layers of κ-phase BETS salts. Ab initio MO and DFT methods with the 6-31G basis sets, i.e. the UHF/6-31G and UB3LYP/6-31G methods, were applied to evaluate effective exchange integrals and the obtained results are summarized in Table 2. The obtained results were −264, −31, −3 and −24 cm^{-1} (UHF); −822, −207, −6, −80 cm^{-1} (UB3LYP) for A, B, p and q, respectively. From the results for both BETS salts we can found that all the evaluated $J_{ab(M)}$ values are negative. These antiferromagnetic values appeared and are dominant because of overlapping between each SOMO. For the all methods the evaluated $J_{ab(M)}$ values for the nearest pair A were very small, showing the especially strong SOMO–SOMO interaction. The $J_{ab(M)}$(B) values for B-type pair are relatively small. On the other hand, the $J_{ab(M)}(q)$ and $J_{ab(M)}(p)$ values turned to be nearly zero in this order. From these tendency it can be concluded that A- and B-type dimers are dominant in this system. The UHF method tends to reproduce small $|J_{ab(M)}|$ values, while the UBLYP method overestimates antiferromagnetic interaction. Thus, the results calculated by UB3LYP are reasonable.

Second, it is important that we treated the J_{ab} values between BETS and $FeCl_4$ molecules as the p–d magnetic interaction between donor and transition metal halides. In order to study magnetic interaction between BETS+ cations and $FeCl_4^-$ anions the pairs which have the shortest intermolecular distance are focused as shown in Fig. 5C. Total spin momentum of septet and quintet are equivalent to the highest and lowest spin states. The J_{ab} values evaluated by UB3LYP and UHF method are 15.2 and −0.101 cm^{-1}, respectively, for pair (a-1), i.e. $FeCl_4^-$(a)(5/2↑)... BETS+(1)(1/2↑ or 1/2↓) as shown in Table 3. The results derived by UB3LYP and UHF methods differ each other. The UB3LYP method reproduced positive value with overestimate J_{ab} values. More extended discussion is feasible if we study another spin structure in pair (a-1-2), for example, $FeCl_4^-$(a)(5/2↑)... BETS+(1)(1/2↑ or 1/2↓)...BETS0(2)(0) and $FeCl_4^-$(a)(5/2↑)... BETS0(1)(0)... BETS+(2)(1/2↑ or 1/2↓).

Next, in order to explain and understand the above conclusions, let us consider the shape of spin densities by graphical representation. Fig. 9A and B illustrate the spin densities for the results calculated by the UB3LYP and UHF methods, where total spin states are septet and quintet. The regions of up (alpha) and down (beta) densities were shown in dark and light gray color and cutoff threshold is set to 0.002. From these results it is found that spin densities in all $FeCl_4^-$ anions are alpha and isotropic. On the other hand, spin densities in $BETS^+$ cations are delocalized and spread over whole atoms without alternation of spin phase. Concerning UB3LYP methods the spin densities for septet and quintet states resemble each other except for whole spin phase in $BETS^+$ cations. There are no spin densities in the H and C atoms in $BETS^+$ cations where Cl atoms in $FeCl_4^-$ anions contact. That might be the reason why only small $|J_{ab}|$ values are evaluated.

In addition, the total charge/spin densities which were summed into molecules 1 and a and are shown in Table 3. From this table it is fount that almost complete distribution of total charge densities on each molecule is successfully accomplished, i.e. about 0.9–1.0 values of negative and positive are expected in $FeCl_4^-$(a) and $BETS^+$(1), respectively. The results derived with both UB3LYP and UHF methods show same tendencies.

Finally, natural orbital (NO) analysis for septet state were carried out in order to study contribution of BETS and $FeCl_4$ molecules to magnetic interaction. In Fig. 10 NO coefficients for each orbital (HOMO, SOMO and LUMO) and their graphical representations are summarized for septet and quintet states by UB3LYP and UHF methods. For the UB3LYP solutions for septet spin state, the occupation number for SOMO(n) ($n = 1, 2, \ldots, 6$) is 1.00000 and each orbital is occupied in one

Table 2
$J_{ab(M)}$ (cm^{-1}) values evaluated by UB3LYP and UHF/6-31G for all donor pairs in κ- and λ-phases BETS, κ-phase BEDT-TTF, TMTTF and TMTSF crystals

	A(1–2)	B(2–5)	p(2–7)	q(2–8)					
κ-$(BETS)_2FeCl_4$	821.8 [a]	206.7	6.5	79.7					
($T = 295$ K) [b]	(263.8) [a]	(31.3)	(2.7)	(24.1)					
κ-$(BEDT\text{-}TTF)_2Cu[N(CN)_2]Cl$	−734	−60	−143	−21					
($T = 127$ K)									
κ-$(BEDT\text{-}TTF)_2Cu[N(CN)_2]Br$	693.2	50.6	157.4	17.8					
($T = 127$ K)	(279.6)	(14.4)	(47.9)	(1.0)					
κ-$(BEDT\text{-}TTF)_2Cu[N(CN)_2]I$	−580	−26	−180	−11					
($T = 127$ K)									
κ-$(BEDT\text{-}TTF)_2Cu(NCS)_2$	−620	−71	−122	−15					
($T = 295$ K)									
	A(1–2)	B(2–3)	C(1–9)	p(1–5)	r(1–6)	q(2–6)	s(2–7)	t(5–9)	(1–11)
λ-$(BETS)_2FeCl_4$			−594.9	−1.7	−39.6	5.0	−2.3	−111.8	0.0
($T = 295$ K)	(−549.1)	(−62.9)	(−149.9)	(10.3)	(−6.3)	(12.2)	(−0.1)	(−33.3)	(0.0)
	(1–5)	(1–2)	(1–3)	(1–4)					
$(TMTTF)_2PF_6$	−682.5	−570.6	−7.4	−14.4					
($T = 4$ K)	(−309.7)	(−244.9)	(−1.4)	(−4.1)					
$(TMTSF)_2PF_6$	−1059.0	−993.2	−18.0	−34.0					
($T = 4$ K)	(−527.1)	(−462.7)							

[a] The UB3LYP/6-31G (UHF/6-31G in parenthesis) methods were employed.
[b] Temperature where the employed crystalline structure was measured.

electron. On the other hand, the occupation numbers for HOMO and LUMO are about 2.0 and 0.0 and hardly contribute intermolecular magnetic interaction through indirect electron correlation correction. The lobes of only SOMO(6) spread over not only $FeCl_4$ but also BETS molecules, though lobes of the other SOMOs are localized only on $FeCl_4$ molecule. From these result it is concluded that the SOMO(6) and degenerated SOMOs play essential role in magnetic interaction.

4.2.2. For λ-phase crystal in $BETS_2FeCl_4$

In this section physical properties for λ-phase BETS salts are discussed in detail. In this crystalline phase another type of donor arrangement is found as shown in

Table 3
$J_{ab(M)}$ (cm^{-1}) values evaluated by UB3LYP and UHF/6-31G methods for $BETS^+$–$FeCl_4^-$ pairs in κ- and λ-phase BETS salts

Pairs	J_{ab} (cm^{-1})	Charge density[c]		Spin density[c]	
		$FeCl_4^-$(a)	$BETS^+$(1)	$FeCl_4^-$(a)	$BETS^+$(1)
in κ-$BETS_2FeCl_4$					
pair (a-1) [$FeCl_4^-$(a) … BETS+(1)]	15.2 [a]	−0.916	0.916	5.07	0.932
	(−0.101) [a]	(−0.991)	(0.991)	(5.00)	(−1.00)
in λ-$BETS_2FeCl_4$					
pair (1-a): $BETS^+$ 1 and below-$FeCl_4^-$	(0.0)				
pair (1-b)	(−0.1)				
pair (1-d)	(−1.7)				
pair (1-e)	(−0.1)				
pair (2-b): $BETS^+$ 2 and below-$FeCl_4^-$	(0.0)				
pair (2-c)	(0.0)				
pair (2-e)	(0.4)				
pair (2-f)	(0.0)				
pair (1-A): $BETS^+$ 1 and above-$FeCl_4^-$	(−9.2)				
pair (1-D)	(0.0)				
pair (2-A): $BETS^+$ 2 and above-$FeCl_4^-$	(0.0)				
pair (2-B)	(−12.7)				
pair (2-D)	(0.0)				
pair (2-E)	(−0.2)				

[a] The UB3LYP/6-31G (UHF/6-31G in parenthesis) methods were employed.

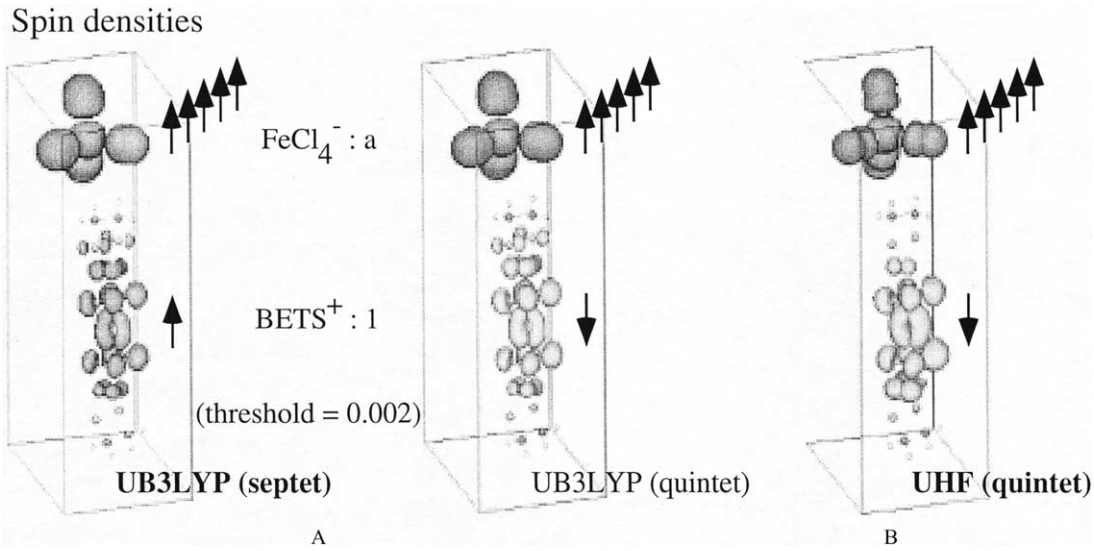

Fig. 9. The calculated spin densities for pair (a-1) in κ-$BETS_2FeCl_4$ by (A) UB3LYP and (B) UHF are showed.

Fig. 6A. The difference in donor orientation in both κ- and λ-phases can be made clear, if we see Fig. 5AFig. 6A. Thus, we treated these systems by evaluating J_{ab} values. The calculated $J_{ab(M)}$ values between two $BETS^+$ cations are also summarized in Table 2. Their molecular notation for each BETS donor are also defined in Fig. 6A. From the results remarkable strong antiferromagnetic interaction is detected in pair A(1–2), C(1–9) and B(2–3), where each BETS molecule is oriented in face-to-face type in one-dimensional alignment. In addition, non-zero interaction is found in the other pairs, where each BETS molecule is oriented in

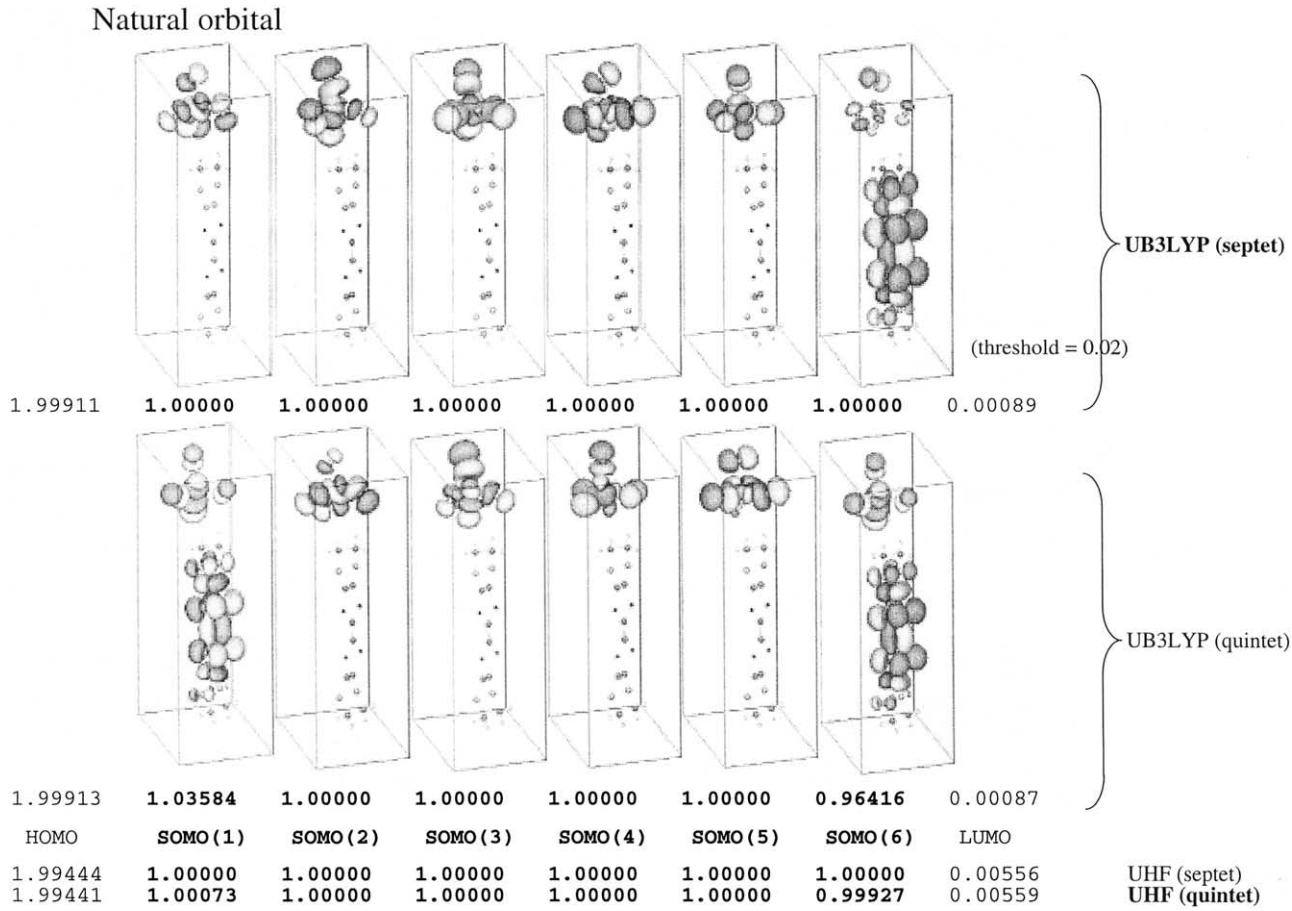

Fig. 10. The natural orbitals and their occupation numbers calculated for pair (a-1) in κ-$BETS_2FeCl_4$ are showed.

side-by-side type. For pair (1–11) J_{ab} values is zero and it is found that its interaction is head-and-tail type.

Second, it is important that we treated the Jab values between $BETS^+$ cation and $FeCl_4^-$ anions. In order to study magnetic interaction between these BETS and $FeCl_4$ molecules, we employed several pairs which have short inter-molecular distance as shown in Fig. 6B. For these pairs the evaluated J_{ab} values are summarized in Table 3, here the results with the UB3LYP method are not listed because of overestimation for J_{ab} values in previous κ-phase system. For pairs (2-B) and (1-A) relatively strong interactions exist, though there are very weak or zero interaction for the other pairs. The difference between the results derived by UB3LYP and UHF methods may occur because of over-stabilization of higher spin state by UB3LYP methods. These interaction between BETS donor and $FeCl_4^-$ anions may cause the external magnetic field effects [32] such as Jaccarino–Peter (JP) effect [33], i.e. revival of superconductivity under high magnetic field. More detailed study are now investigating.

4.3. BEDT-TTF complexes for several counter ions

In addition to κ-phase BETS salts, the studies for κ-phase BEDT-TTF salts are very interesting. Here, several κ-phase salts were mainly studied, though many λ-phase BEDT-TTF salts are also known. We evaluate J_{ab} values between two donor molecules in two-dimensional layer as shown in Fig. 7. The calculated the $J_{ab(M)}$ values between two BEDT-TTF cations are also summarized in Table 2. Here, our theoretical calculation were applied for complexes **3a**, **3b**, **3c** and **4**. From these results the all obtained $J_{ab(M)}$ values are negative. For the all methods the evaluated $J_{ab(M)}$ values for the nearest pair A was very small, showing the especially strong SOMO–SOMO interaction. The $J_{ab(M)}$(B) values for B-type pair are relatively small. On the other hand, the $J_{ab(M)}(q)$ and $J_{ab(M)}(p)$ values turn to be nearly zero in this order. From these tendency it can be concluded that A-, p- and B-type dimers are dominant. The UHF method tends to reproduce small $|J_{ab(M)}|$ values, while the UBLYP method overestimates antiferromagnetic interaction. On the other hand, the results calculated by UB3LYP are reasonable. These tendency is commonly found to κ-phase BETS salts as mentioned above.

4.4. TMTTF and TMTSF complexes

In this section we study magnetic interaction in another type of donor complex, i.e. J_{ab} values in chain of TMTTF and TMTSF donors. Same procedures of theoretical calculations were carried out for TMTTF and TMTSF donors. The results were summarized in Table 2. First, from the results for 5 as TMTTF salts, it is found that all the $J_{ab(M)}$ values are negative and the $J_{ab(M)}$ value for pair (1–5) is the largest, though the value for pair (1–2) is also large. The interaction in the nearest neighbor pairs and the second nearest neighbor pairs is remarkable and showing the strong magnetic coupling. A little dimerization along donor chain occurs and leads difference between two $J_{ab(M)}$ values. On the other hand, the $J_{ab(M)}$ values for pairs (1–3) and (1–4) are not remarkable. From these values, one-dimensional network through face-to-face stacking chain are very dominant. On the other hand, the results for **6** as TMTSF salts very similar tendency to **5** is found except for stronger interaction.

For our future study, in order to derive more detailed information several large scale calculations by ab initio methods for four molecular clusters will be carried out. Theoretical calculations in cluster molecules are composed of many number of atoms and need very large CPU-time. The contribution of each electronic configuration to charge ordering state will be analyzed among several cluster models. These calculations depended by ab initio HF and DFT methods will successfully explain magnetic interaction.

5. Estimation of other values from the previous J_{ab} values

5.1. Effective parameters (t_{ab}, U_{eff}) with numerical fitting

In addition to effective exchange integrals (J_{ab}) in sheet of donors, the other effective magnetic parameters (s_{ab}, t_{ab} and U_{eff}) can be evaluated with the calculated $J_{ab(M)}$ values. In our studies, we treated only the systems for BEDT-TTF and BETS salts, though our theoretical treatment is also feasible for the system for TMTTF and TMTSF salts. In these systems overlap integrals (s_{ab}) between SOMOs for all pairs (A, B, p and q) in κ-phase BEDT-TTF and BETS salts (**1a**, **3a**, **3b**, **3c** and **4**) are calculated by R(O)HF, UHF-NO, UB3LYP, UBLYP and hybrid-DFT (UB2LYP) methods with the 6-31G basis sets. In Fig. 11B the s_{ab} (x-axis) and J_{ab} (y-axis) values with UB3LYP method are plotted so as to examine relationship between these integrals. Here, the all data for both BEDT-TTF and BETS salts were commonly employed for both BETS and BEDT-TTF cases in order to improve numerical reliability. The curvature can be obtained with fitting technique into Eq. (10) and we can suppress the divergence between fitting curvature and the data. Under the equation $t_{ab} = \beta s_{ab}$ and $U_{eff} = U_{aa} - V_{ab}$, the optimized values were successfully obtained as summarized in Table 4. The $c2$ and R data to judge the quality of the fit were evaluated to be $c2 = 11\,784$, $R = 0.99608$ (unit: cm^{-1}, 1 eV = 8066 cm^{-1}). In addition, all t_{ab} values can be also evaluated with both the sab value and the parameter β with Eq. (9). Though variation of t_{ab} values is commonly small

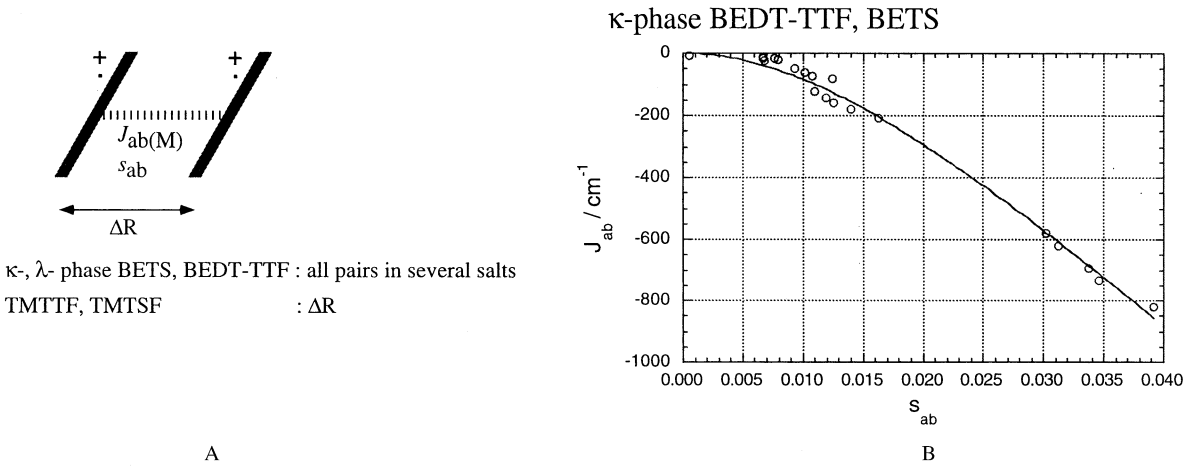

Fig. 11. (A) Many sampling models for J_{ab} and s_{ab} values is needed to obtain t_{ab} and U_{eff} values. (B) All pairs (J_{ab}, s_{ab}) with the UB3LYP method in κ-phase BEDT-TTF and BETS salts were plotted and parameter fitting with these points were carried out.

for all theoretical methods and the U_{eff} values depend on computational methods. The U_{eff} values by the UHF method is larger (1.68 eV) and the values by the UBLYP method is relatively smaller (0.138 eV). The UB2LYP method as hybrid-DFT method gives moderate U_{eff} values. Large electron correlation in this system affect the U_{eff} values obtained with these methods.

5.2. Dimensionality of interaction

In the previous sections we determine all $J_{ab(M)}$ values. In this section, let us consider another effective exchange integrals, i.e. $J_{ab(D)}$, values between two dimers in the condition of one hole doping per one dimer (namely, two holes in four molecules). Nevertheless,

Table 4
All effective magnetic parameters evaluated with parameter fitting

	J_{ab} (cm^{-1})	s_{ah}	t_{ab} (eV)	β (eV) [a]	U_{eff} (eV) [a]	x [b]	
in κ-$BETS_2FeCl_4$							
UHF/6-31G	−264	0.0336	0.174	5.19	1.68	0.104	(pair A)
	−31.3	0.0109	0.057	↑	↑	0.034	(pair B)
	−2.72	0.0005	0.003	↑	↑	0.002	(pair p)
	−24.1	0.0126	0.065	↑	↑	0.039	(pair q)
UB2LYP	−543	0.0383	0.161	4.21	0.603	0.267	(pair A)
UB3LYP	−822	0.0392	0.176	4.50	0.374	0.471	(pair A)
	−207	0.0163	0.073	↑	↑	0.195	(pair B)
	−6.46	0.0006	0.003	↑	↑	0.008	(pair p)
	−79.7	0.0124	0.056	↑	↑	0.150	(pair q)
UBLYP [c]	−1218	0.0401	0.175	4.36	0.138	1.268	(pair A)
in κ-$(BEDT\text{-}TTF)_2FeCl_4$							
UHF/6-31G	−280	0.0324	0.168	5.19	1.68	0.100	(pair A)
	−14.4	0.0089	0.046	↑	↑	0.027	(pair B)
	−47.9	0.0116	0.060	↑	↑	0.036	(pair p)
	−1.09	0.0052	0.027	↑	↑	0.016	(pair q)
UB2LYP	−479	0.0334	0.141	4.21	0.603	0.234	(pair A)
UB3LYP	−693	0.0338	0.152	4.50	0.374	0.406	(pair A)
	−50.6	0.0093	0.042	↑	↑	0.112	(pair B)
	−157	0.0126	0.057	↑	↑	0.152	(pair p)
	−17.8	0.0076	0.034	↑	↑	0.091	(pair q)
UBLYP [c]	−1004	0.0337	0.147	4.36	0.138	1.065	(pair A)

[a] The J_{ab} and s_{ab} values calculated for all pairs A, B, p and q in all κ-phase crystals were employed in order to evaluate effective parameters.
[b] $x = t_{ab}/U_{eff}$.
[c] The closed shell solution (RBLYP) for lower spin state, because of SCF convergence failure.

theoretical calculations for these clusters need huge CPU-time and convergence difficulty, though ab initio calculations to evaluate effective exchange integrals for four molecules with two hole doping is desired for more advanced discussion.

Here, the interaction in the two-holes-doped tetramer can be approximately regarded as the interaction between two dimer cations with each one hole. We assume that each hole is introduced into antibonding orbital in dimer and complete delocalization of molecular orbital is realized. In this calculation model $J_{ab(D)}$ values between two dimers is a half of the $J_{ab(M)}$ values ($J_{ab(D)} \simeq J_{ab(M)}/2$) as shown in Eq. (6). On the other hand, in the case that hole localize completely into one molecule, that is, the charge ordering condition, $J_{ab(D)}$ values will be equal to zero or whole $J_{ab(M)}$ values.

For κ-phase BEDT-TTFT and BETS salts remarkable dimer structure is found and our treatment is feasible. Thus for these systems the derived results for $J_{ab(D)}$ values derived are summarized in Table 5, where indices for each cluster which is combination of two dimers are defined in Fig. 5AFig. 7. In addition, for λ-phase BETS salts have another dimer structure and same treatment is feasible. On the other hand, for TMTTF and TMTTF salts where very weak dimerization is found the $J_{ab(D)}$ values can be evaluated. These values were used only for rough discussion and of source cluster calculation is preferred for more accurate and detailed discussion

From these result for BEDT-TTF and BETS systems, the calculated $J_{ab(D)}$ values are in the range: about $-10--100$ cm^{-1}. It is found that the inter-spin interaction obtained by the ab initio calculations is square planar for BEDT-TTF, since our calculation indicate the $|J_{ab(D)}(1)|$ and $|J_{ab(D)}(2)|$ values (bold lines) are larger than $|J_{ab(D)}(3)|$ values (broken lines) as shown in Fig. 7. The disparity in each $J_{ab(D)}$ value for BEDT-TTF salts (**3a**, **3b**, **3c** and **4**) is very small and there is possibility of organic superconductor for these crystals. On the other hand, it is found that the spin lattice for BETS plane is linear, since $|J_{ab(D)}(3)|$ values are larger than $|J_{ab(D)}(1)|$ and $|J_{ab(D)}(2)|$ values as shown in Fig. 5A. Though two-dimensional networks through paths 1 and 2 are essential for BEDT-TTF complexes, one-dimensional networks are more dominant for BETS complexes. On the other hand, from these results for TMTTF and TMTSF, one-dimensional interaction is expected as shown in Fig. 8B.

Table 5
$J_{ab(D)}$ values evaluated for κ-phase crystals of BEDT-TTF and BETS salts

Compounds	$J_{ab(D)}(1)$ (cm^{-1})	$J_{ab(D)}(2)$	$J_{ab(D)}(3)$
κ-(BETS)$_2$FeCl$_4$	−39.9 [a]	−39.9	−103.3
	(−12.1) [a]	(−12.1)	(−15.6)
κ-(BEDT-TTF)$_2$Cu[N(CN)$_2$]Cl	−71.5	−71.5	−30.0
κ-(BEDT-TTF)$_2$Cu[N(CN)$_2$]Br	−78.7	−78.7	−25.3
	(−24.0)	(−24.0)	(−7.2)
κ-(BEDT-TTF)$_2$Cu[N(CN)$_2$]I	−90.0	−90.0	−13.0
κ-(BEDT-TTF)$_2$Cu(NCS)$_2$	−61.0	−61.0	−35.5

[a] The UB3LYP/6-31G (UHF/6-31G in parenthesis) methods were employed.

5.3. Estimation for TSC values

Previous Eq. (12) is useful for estimating T_{SC} with J_{ab} values. Thus, we here estimate T_{SC} values for these systems. Before we apply this equation to these donor systems, we think CuO system is suitable system for introduction. If we permit our very rough estimation, T_{SC} can be estimate by magnitude of J and J':

$J,\ J' \approx -1000\ \text{cm}^{-1} \quad T_{SC} = 100\ \text{K}$

(CuO; high-T_C SC)

In Eq. (12) the parameter x indicates densities of hold doing, i.e. for example $x = 0.5$ indicates 1 hole in 2 donors: $(D_2)^+$. Thus we can use the $J_{ab(D)}$ values estimated in the above section. From these results it is found that J values for the BEDT-TTF, TMTTF and TMTSF salts support this estimation. Only for BETS, divergency from two-dimensional interaction networks lead small T_{SC} values, though magnitude of J values are not so different from those for BEDT-TTF. For TMTTF and TMTSF donors, weak interchain interaction for pairs (1–3) and (1–4) is not negligible, since lack of these interaction makes T_{SC} vanish. If we permit our very rough estimation, T_{SC} can be classified by magnitude of J and J':

$J,\ J' \approx -100 \quad T_{SC} \simeq 10\ K$ (BEDT-TTF; highest)

$J \approx -100,\ J \approx -1 \quad T_{SC} \approx 1\ \text{K}$

(TMTTF, TMTSF; 1D)

These procedure is regarded as rough treatment, but it is very useful tool to approximately determine T_{SC} temperature.

6. Discussion

Our previous studies enabled us to obtain the detailed magnetic parameters with the theoretical calculations, that is, all magnetic parameters (effective exchange integral (J_{ab}), transfer integral (t_{ab}), etc.) between donors with the molecular orbital calculation are successfully evaluated. In our studies these ab initio HF and DFT methods can directly determine effective parameters, though in the other groups the extended Hükel band models usually provide Fermi surfaces for organic conductors and band pictures have been used for explanations of electronic properties.

From the result, it is found that two- (Fig. 5A) and quasi-one- (Fig. 7) dimensional interaction are dominant for κ-phase of BEDT-TTF and BETS donor layers, respectively. This feature deduce that T_{SC} of BEDT-TTF salts is higher than that of BETS salts, though absolute values of intermolecular interaction in BEDT salts are larger than that in BEDT-TTF salts because of larger orbital overlap on selenium atoms. On the other hand for λ-phase of BETS donor layers, interaction along chains is dominant. For both TMTTF and TMTSF salts one-dimensional interaction is expected as shown in Fig. 8B.

For our future detailed discussion, we will carry out larger size calculations in order to study partial hole doping. The the UNO-CASCI and CASSCF methods are suitable to treat delocalization of hole densities between not only two but also four molecules. We will also adapt the obtained effective parameters to the phase-diagrams of spin clusters, which were already obtained by the other researchers. We expect that these theoretical studies successfully explain the mechanism of organic superconductive systems and feed back to experimental crystal design with physical pressure effect and chemical doping.

Acknowledgements

This work has been supported by a Grant-in-Aid for Scientific Research on Priority Areas (Nos. 14204061 and 13740396) from Ministry of Education, Culture, Sports, Science and Technology, Japan.

References

[1] J.G. Bednort, K.A. Muller, Z. Phys. 64 (1986) 189.
[2] W.E. Pickett, Rev. Mod. Phys. 61 (1989) 433.
[3] A.P. Kampf, Phys. Reps. 249 (1994) 219.
[4] W. Brenig, Phys. Rep. 251 (1995) 153 (and references therein).
[5] M. Imada, A. Fujimori, Y. Tokura, Rev. Mod. Phys. 70 (1998) 1040.
[6] K. Yamaguchi, Int. J. Quant. Chem. 37 (1990) 167.
[7] H. Kobayashi, A. Kobayashi, P. Cassoux, Chem. Soc. Rev. 29 (2000) 325.
[8] H. Akutsu, E. Arai, H. Kobayashi, H. Tanaka, A. Kobayashi, P. Cassoux, J. Am. Chem. Soc. 119 (1997) 12681.
[9] H. Akutsu, K. Kato, E. Ojima, H. Kobayashi, H. Tanaka, A. Kobayashi, P. Cassoux, Phy. Rev. B58 (1998) 9294.
[10] H. Tanaka, A. Kobayashi, A. Sato, H. Akutsu, H. Kobayashi, J. Am. Chem. Soc. 121 (1999) 760.
[11] K. Miyagawa, A. Kawamoto, Y. Nakazawa, K. Kanoda, Phys. Rev. Lett. 75 (1995) 1174.
[12] K. Kanoda, Physica, C282–287 (l997) 290, Hyperfine Interaction 104 (1997) 235.
[13] T. Kawakami, T. Taniguchi, Y. Kitagawa, Y. Takano, H. Nagao, K. Yamaguchi, Mol. Phys., in press.
[14] G. Saito, S. Kagoshima (Eds.), The Physics and Chemistry of Organic Superconductors, Springer, Berlin, 1990.
[15] J.M. Williams, et al., Prog. Inorg. Chem. 35 (1987) 51.
[16] U. Geiser, A.J. Schults, H.H. Wang, D.M. Watkins, D.L. Stupka, J.M. Williams, J.E. Schirber, D.L. Overmyer, D. Jung, J.J. Novoa, M.H. Whangbo, Physica C174 (1991) 475.
[17] T. Mori, Bull. Chem. Soc. Jpn. 71 (1998) 2509.
[18] T. Mori, H. Mori, S. Tanaka, Bull. Chem. Soc. Jpn. 72 (1999) 179.
[19] T. Soda, Y. Kitagawa, T. Onishi, Y. Takano, Y. Shigeta, H. Nagao, Y. Yoshioka, K. Yamaguchi, Chem. Phys. Lett. 319 (2000) 223.
[20] T. Onishi, T. Soda, Y. Kitagawa, Y. Takano, Y. Daisuke, S. Takamizawa, Y. Yoshioka, K. Yamaguchi, Mol. Cryst. Liq. Cryst. 343 (2000) 133.
[21] K. Yamaguchi, M. Nakano, H. Namimoto, T. Fueno, J.J. Appl. Phys. 27 (l988) L1835; 27 (1989) L479; 28 (1989) L672.
[22] Y. Imamura, S. Ten-no, K. Yonemitsu, Y. Tanimura, J. Chem. Phys. 111 (1999) 5986.
[23] A. Fortunelli, A. Painelli, Phys. Rev. B55 (1997) 16088.
[24] H. Kino, H. Kontani, J. Phys. Soc. Jpn. 67 (1998) 3691.
[25] Oshima et al. Phys. Rev. B38 (1988) 938
[26] H. Kobayashi, H. Tomita, T. Naito, A. Kobayashi, F. Sakai, T. Watanabe, P. Cassoux, J. Am. Chem. Soc. 118 (1996) 368.
[27] C. Hotta, H. Fukuyama, J. Phy. Soc. Jpn. 69 (2000) 2577.
[28] K.D. Carlson, U. Geiser, A.M. Kini, H.H. Wang, L.K. Montgomery, W.K. Kwok, M.A. Beno, J.M. Williams, C.S. Cariss, G.W. Crabtree, Inorg. Chem. 27 (1988) 965.
[29] P. Day, M. Kurmoo, T. Mallh, I.R. Marsden, R.H. Friend, F.I. Pratt, W. Hayes, D. Chasseau, G. Bravie, L. Oucasse, J. Am. Chem. Soc. 114 (1992) 10722.
[30] K. Yamaguchi, Y. Takahara, T. Fueno, K. Nasu, J.J. Appl. Phys. 26 (l987) L1362; 26 (1987) L2037; 27 (l987) L509.
[31] M.J. Frisch et al., J.A. Pople, GAUSSIAN 98, Gaussian, Inc.
[32] S. Uji, et al., Nature 410 (2001) 908.
[33] V. Jaccarino, M. Peter, Phys. Rev. Lett. 9 (1962) 290.